Intravascular detection of inflamed atherosclerotic plaques using a fluorescent photosensitizer targeted to the scavenger receptor

Ahmed Tawakol[a], **Ana P. Castano**[b,c], **Faten Gad**[†,b,c], **Touqir Zahra**[b,c], **Gregory Bashian**[a], **Raymond Q. Migrino**[d], **Atosa Ahmadi**[b], **Jeremy Stern**[b], **Florencia Anatelli**[b,c], **Stephanie Chirico**[b], **Azadeh Shirazi**[b], **Sakeenah Syed**[d], **Alan J. Fischman**[d], **James E. Muller**[a], and **Michael R. Hamblin**[b,c,e]

[a]Department of Medicine (Cardiac Unit), Massachusetts General Hospital, Boston, MA, 02114

[b]Wellman Center for Photomedicine Massachusetts General Hospital, Boston, MA, 02114. hamblin@helix.mgh.harvard.edu; Fax: 617-726-8566; Tel: 617-726-6182

[c]Department of Dermatology, Harvard Medical School, Boston, MA

[d]Department of Radiology, and Nuclear Medicine, Massachusetts General Hospital, Boston, MA, 02114

[e]Harvard-MIT Division of Health Sciences and Technology, Cambridge, MA

Abstract

Inflammation plays an important role in the pathophysiology of atherosclerotic disease. We have previously shown that the targeted photosensitizer chlorin (e_6) conjugated with maleylated albumin (MA-ce6) is taken up by macrophages *via* the scavenger receptor with high selectivity. In a rabbit model of inflamed plaque in New Zealand white rabbits *via* balloon injury of the aorto-iliac arteries and high cholesterol diet we showed that the targeted conjugate showed specificity towards plaques compared to free ce6. We now show that an intravascular fiber-based spectrofluorimeter advanced along the -iliac vessel through blood detects 24-fold higher fluorescence in atherosclerotic vessels compared to control rabbits ($p < 0.001$ ANOVA). Within the same animals, signal derived from the injured iliac artery was 16-fold higher than the contralateral uninjured iliac ($p < 0.001$). Arteries were removed and selective accumulation of MA-ce6 in plaques was confirmed using: (1) surface spectrofluorimetry, (2) fluorescence extraction of ce6 from aortic segments, and (3) confocal microscopy. Immunohistochemical analysis of the specimens showed a significant correlation between MA-ce6 uptake and RAM-11 macrophage staining ($R = 0.83$, $p < 0.001$) and an inverse correlation between MA-ce6 uptake and smooth muscle cell staining ($R = -0.74$, $p < 0.001$). MA-ce6 may function as a molecular imaging agent to detect and/or photodynamically treat inflamed plaques.

Introduction

Cardiovascular disease remains the leading cause of morbidity and mortality in the United States, largely due to events caused by the sudden rupture of an atherosclerotic plaque.[1] Such rupture-prone plaques are characterized by a large necrotic lipid cores, thin fibrous caps, and dense macrophage infiltration.[2] An attractive target for both detection and therapy of these

Correspondence to: Michael R. Hamblin.

[†]Deceased.

plaques is the local inflammatory cells (particularly activated macrophages) that contribute significantly to plaque instability.[3]

Photodynamic therapy (PDT) uses non-toxic photosensitizers (PS) that can be photoactived upon the delivery of light.[4] Exposure of the PS to light raises the PS molecule to an excited state that, depending on the dose and wavelength of light used, can lead predominantly to: (1) the generation of cytotoxic reactive oxygen species, or (2) the emission of fluorescence light. [4] PDT is currently approved for the treatment of esophageal and lung cancer and age-related macular degeneration.[5] Its application to atherosclerotic disease is currently under investigation.[6]

Recently molecular imaging approaches[7] have been suggested to improve the detection, characterization, and image the processes occurring within the atherosclerotic plaque,[8] with the specific aims of quantifying the levels of inflammation[9] and predicting the likelihood of rupture.[10] Many different targets within plaques have been proposed as markers of vulnerability, including matrix-metalloproteinase activity,[9,11] inflammation as measured by positron emission tomography,[12] and the macrophage content and activation state.[13] Optical detection by such techniques as fluorescence is preferred for molecular imaging technologies due to its relative safety (lack of radioisotopes) and low cost compared to MRI and PET.[14] Possible disadvantages of optical imaging however include its invasive nature and difficulties faced by absorption and scattering of light by blood.

Photosensitizers can be selectively delivered to target tissues by using covalent conjugates between PS and macromolecular carriers with targeting properties.[4] An attractive receptor target within inflamed atherosclerotic plaques is the macrophage class A Type-I scavenger receptor, (SR-As), high capacity membrane glycoproteins that are confined mainly to tissue macrophages and related cell types.[15] The SR-A play an important role in the pathophysiology of atherosclerosis,[16,17] by mediating the uptake of low density lipoprotein (LDL) uptake by human monocyte-derived macrophages,[18] and enhancing their transformation into lipid-laden foam cells.[19]

Well-defined ligands of the SR-A include modified or oxidized LDL and maleylated serum albumin.[20] We have previously demonstrated that the PS chlorin (e6) could be covalently attached to maleylated serum albumin to form MA-ce6.[21] We demonstrated that the MA-ce6 conjugate is recognized by SR-A, and concentrates in macrophages *in vitro* with high specificity, and that subsequent photoactivation results in macrophage-specific toxicity.[21,22] By using this conjugate it was possible to specifically target macrophages that are present in high numbers in mouse tumors especially by intratumoral injection.[23] Using a rabbit model of macrophage-rich arterial atherosclerotic plaque we showed that intravenous injection of MA-ce6 could lead to localization of fluorescent ce6 in macrophage-rich atherosclerotic lesions extracted from sacrificed rabbits.[24] The optimum time for accumulation in the plaques was 24 hours after injection, and this combination of PS and incubation time was superior to MA-ce6 at 6 hours and to free ce6 at either 6 or 24 hours. We now asked whether this technique could be used as a diagnostic or detection procedure. We tested whether the injected targeted conjugate did in fact localize in macrophages in the arterial wall as determined by correlation of fluorescence from frozen sections removed at necroscopy, with immunohistochemical staining for the macrophage marker RAM11. Moreover we also correlated the red fluorescence with the absence of smooth muscle cells by IHC for alpha-actin.

Materials and methods

Preparation of conjugate

The scavenger-receptor-targeted conjugate between maleylated albumin and ce6 was prepared as previously described.[21] Briefly the *N*-hydroxy succinimide ester of ce6 (Frontier Scientific Inc, Logan UT) was added to bovine serum albumin (Sigma, St. Louis, MO) in $NaHCO_3$ buffer, followed by the addition of solid maleic anhydride. The conjugate was then purified by repeated precipitation from aqueous solution by addition of acetone followed by dialysis, and characterized by polyacrylamide gel electrophoresis and absorption and fluorescence spectrophotometry.

Experimental atherosclerotic lesions

The protocol was approved by the animal care and use committee of the Massachusetts General Hospital and complies with National Institutes of Health approved guidelines. Fifteen male New Zealand White rabbits weighing 2.5–3.0 kg (Charles River Breeding Laboratories) were maintained on a 2%cholesterol–6% peanut oil diet (ICN Biomedical, Costa Mesa, CA) for 3–6 months. After 1week of the hyperlipidemic diet, -iliac endothelial denudation was achieved using a modified Baumgartener technique.[25] Briefly, each animal was anesthetized with a mixture of ketamine and xylazine (100 mg ml^{-1}, 10 : 1 vol/vol; 1.5–2.5 ml subcutaneous) and the right femoral artery was isolated. A 4F Fogarty embolectomy catheter (12-040-4F; Edwards Laboratories, Santa Ana, CA) was introduced through an arteriotomy and advanced to the level of the diaphragm. The catheter was inflated to a pressure of approximately 3 psi above the balloon inflation pressure, and withdrawn for a distance of 3 cm and then re-advanced 3 cm. The procedure was repeated 5 times. The area of injury produced was located in the lower thoracic and mid-abdominal aorta together with the right iliac artery that sustained injury due to passage of the deflated balloon. The femoral artery was then ligated, and the wound closed. The rabbits were allowed to recover from anesthesia and then returned to their cages. Seven untreated male New Zealand White rabbits fed standard chow served as controls.

Photosensitizer injection

Photosensitizer was administered to the animals three to six months after aortic denudation injury. Animals were anesthetized by IM injection of ketamine and xylazine (50 and 5 mg kg^{-1}) after an overnight fast. Thereafter, MA-ce6 (2 mg kg^{-1} of ce6 equivalent in 10 mL 5% dextrose) was administered intravenously (ear vein) over a 2-minute period.

Assessment of Ce6 localization

Intravascular and biodistribution measurements were performed 24-hours after photosensitizer injection, following euthanasia of the animals with an overdose of sodium pentobarbital (200 mg kg^{-1}). Accumulation of MA-Ce6 was assessed: (1) *in situ* (through blood) using an intravascular probe, (2) *ex vivo* by surface fluorescence from aortic segments and subsequent fluorescence extraction of ce6 from samples, and (3) with confocal microscopy.

Intravascular localization of conjugate by fiber-based spectrofluorimeter

A single-fiber based spectrofluorimeter system for intravascular fluorescence detection was constructed. A nitrogen laser pumped dye-laser system (models VSL337ND and D220, Laser Sciences Inc., Franklin, MA) operating at 400 nm was coupled with a 400 µm internal diameter fiber with a flat polished end. Reflected light at and fluorescence from the tissue in the range 650–800 nm was collected by the fiber and spectrally dispersed using an imaging spectrograph (SpectraPro, 150, Roper Scientific, Princeton, NJ). A 650 nm longpass filter was used to exclude tissue autofluorescence and exciting light. A gated, intensified CCD array (PI-Max, Roper Scientific, Princeton, NJ) was used for detection. The spectrograph was equipped with

a 25 µm wide input slit and a 150 gr mm^{-1} grating blazed at 450 nm. The spectra obtained from ten laser pulses were averaged for each measurement. A background spectrum (fiber in air) was obtained and subtracted from averaged fluorescence spectra. The fluorescence excitation maximum of ce6 is 404 nm and the emission peaks at 660 nm.

Intravascular fluorescence measurement (through blood)

The thorax and abdomen were surgically exposed and intravascular access obtained by arteriotomy approximately 1 cm above the aorto-iliac bifurcation. The fiber optic catheter was inserted through the arteriotomy and advanced to the aortic arch. Thereafter, measurements in triplicate were performed in the thoracic and abdominal aorta as the fiber was pulled-back towards the aortic incision. The artery was gently compressed with a finger to ensure good contact between the fiber tip and the arterial wall. The fiber was then re-oriented and advanced to the lower aorta together with the uninjured and injured iliac arteries for additional measurements.

Ex situ measurements

The aorta and iliac arteries were then removed *en block*, from the level of the aortic arch to 1.5 cm distal to the iliac bifurcation. After removal of adherent adventitial tissue the aorta was sub-divided and segments corresponding to the thoracic aorta, abdominal aorta, injured- and un-injured iliac arteries identified. Biodistribution of MA-Ce6 within the vascular segments was subsequently determined by surface fluorescence and extraction techniques (described below). Additionally, a ring (3 mm) was excised from each vascular specimen (above), was added to optimum cutting temperature embedding compound (Sakura Finetek USA Inc, Torrance, CA) and snap frozen in liquid nitrogen for subsequent confocal microscopy and immunohistochemical analysis.

Surface fluorescence measurements

Vascular segments were longitudinally incised, moistened with PBS and placed on a black metal plate with intimal side exposed for determination of surface fluorescence. The intimal surface of each vascular segment was examined by spectrofluorimetry using a fiber-bundle based double monochromator spectrofluorimeter (Skin Scan, Spex Industries, Edison, NJ) placed in contact with the tissue. Emission spectra (excitation 400 nm, emission 580–720 nm) were collected every 3 mm across the entire area of the exposed intimal surface.

Fluorescence quantification by extraction from tissue samples

The arterial segments were added to 3 mL of 1 M NaOH–0.2% SDS and homogenized with a Powergen homogenizer for 30 s on ice (Probe model 15-338-2306, Fisher Scientific, Pittsburgh, PA). Homogenates were measured in a spectrofluorimeter (Fluoromax 3, Spex Industries). The peak height of the fluorescence emission (between 658 and 664 nm) was measured (excitation at 400 nm, emission scanned from 580–720 nm). The quantity of MA-Ce6 in the tissue sample was determined by multiplying the fluorescence emission by a constant determined from calibration curves prepared from known amounts of MA-Ce6 homogenized with similar weights of non-fluorescent arterial tissue. Fluorescence within the homogenates was expressed as micromoles equivalent of ce6 per gram of tissue.

Confocal fluorescence microscopy and histology

The aortic rings were snap-frozen in liquid nitrogen and 10 µm frozen sections were prepared. These were examined by laser scanning confocal fluorescence microscopy to detect the tissue distribution of the ce6. The red intracellular fluorescence from ce6 together with green tissue autofluorescence was imaged in the frozen tissue sections. A Leica DMR confocal laser fluorescence microscope (Leica Mikroskopie und Systeme GmbH, Wetzler, Germany)

(excitation 488 nm argon laser) and 4×–40× air immersion lens or a 100× oil immersion objective was used to image at a resolution of 1024×1024 pixels. Two channels collected fluorescence signals in either the green range (580 nm dichroic mirror plus 530 nm (±10 nm) bandpass filter) or the red range (580 nm dichroic mirror plus 590 nm longpass filter) and were displayed as false color images. These channels were overlaid using TCS NT software (Version 1.6.551, Leica Lasertechnik, Heidelberg, Germany) to allow visualization of overlap of red and green fluorescence. These sections were also stained by conventional H&E staining and Verhoeff's stain for elastic lamina.[26]

Immunohistochemical analysis was carried out on adjacent frozen sections using the primary monoclonal anti-bodies; mouse anti-rabbit macrophage, clone RAM11, (Labvision Neomarkers Corp, Fremont, CA) at a dilution of 1 : 500, and mouse anti-rabbit alpha smooth-muscle actin, clone HHF35 (Signet Laboratories, Dedham, MA) at a dilution of 1 : 800. Secondary biotinylated antibodies and peroxidase detection reagents (Vectastain ABC Kit Mouse IgG, Vector Laboratories, Burlinghame, CA) were used to develop the color. Quantitation of brown immunohistochemistry or red fluorescence in TIFF files was carried out by color segmentation using IP Lab software (Scanalytics Inc, Fairfax, VA).

Statistical methods

Data were analyzed using SPSS for Windows version 13.0. Continuous parameters are reported as the mean ± SD. Four primary ANOVA analyses were conducted, for values of: (1) intravascular fiber-based spectrofluorimetry, (2) surface spectrofluorimetry, (3) fluorescence extraction of samples from aortic segments, and (4) confocal microscopy, (each for differences between atherosclerotic and control animals). We applied a Bonferroni correction[27] to the alpha, such that a p value of <0.0125 was considered significant for the primary ANOVA analyses. We subsequently looked for pairwise differences only if the primary ANOVA analysis was significant. For those analyses, the differences between two means were assessed for significance by the two-tailed Students' t test assuming equal or unequal variances of the standard deviations as appropriate. A p value of <0.05 was considered significant for those analyses. Pearson's method[28] was used to assess the correlation between MA-ce6 uptake (confocal fluorescence microscopy) and histopathological measures (RAM-11 and smooth muscle actin staining).

Results

Intravascular detection of conjugate fluorescence

The mean spectrofluorimetric signal derived from the intravascular catheter (through blood) was significantly increased in the aorto-iliac vessel of atherosclerotic rabbits ($n = 15$) compared to the corresponding sections of aorta from control rabbits ($n = 7$, $p < 0.001$ ANOVA atherosclerotic animals *vs.* controls, Fig. 1). The spectrofluorimetric signal detected within the balloon-injured iliac arteries of atherosclerotic animals was approximately 24-fold higher than the corresponding segment in control animals (10010 ± 3050 *vs.* 410 ± 60 AU, atherosclerotic *vs.* control, respectively, $p < 0.001$). A similar difference was observed when injured and un-injured iliac vessels were compared with in the same animal ($10010 \pm 3\,050$ *vs.* 620 ± 240 AU, injured *vs.* non-injured iliac vessel, respectively, $p < 0.02$).

Ex vivo surface fluorescence measurements

The results of the *ex situ* surface spectrofluorimetry measurements paralleled those of the intravascular measurements. The mean surface spectrofluorimetric signal was significantly increased in the aorto-iliac vessel of atherosclerotic rabbits compared to the corresponding sections of aorta from control rabbits ($p < 0.001$ ANOVA atherosclerotic animals *vs.* controls, Fig. 2). The spectrofluorimetric signal detected within the balloon-injured iliac arteries of

atherosclerotic animals was approximately 21-fold higher than the corresponding segment in control animals (24.2 ± 3.0 *vs.* 1.2 ± 0.3 AU, atherosclerotic *vs.* control, respectively, $p < 0.001$). A similar difference was observed when injured and un-injured iliac vessels were compared within the same animal (24.2 ± 3.0 *vs.* 2.7 ± 0.4 AU, injured *vs.* non-injured iliac vessel, respectively, $p < 0.001$).

Fluorescence quantification by extraction from tissue samples

The data followed the same trends for fluorescence quantification by extraction from tissue samples. The tissue concentration of MA-ce6 was significantly increased in all sections from atherosclerotic rabbits ($n = 15$) compared to the corresponding sections of aorta from control rabbits injected with conjugate ($n = 7$, $p < 0.001$ ANOVA atherosclerotic animals *vs.* controls). MA-ce6 concentration within the balloon-injured iliac arteries of atherosclerotic animals was approximately 33-fold higher than the corresponding segment in control animals (16.4 ± 7.1 *vs.* 0.5 ± 0.3 nmol ce6 equiv (g tissue)$^{-1}$, $p < 0.03$, atherosclerotic *vs.* control, respectively, Fig. 3). A similar difference was observed when MA-ce6 concentration in injured and un-injured iliac vessels were compared within the same animal (16.4 ± 7.1 *vs.* 0.6 ± 0.1 nmol ce6 equiv (g tissue)$^{-1}$, $p < 0.04$, injured *vs.* non-injured iliac vessel, respectively).

Confocal fluorescence microscopy and immunohistochemistry

Representative confocal fluorescence micrographs and their corresponding immunohistochemical macrophage stains (RAM-11) are shown in Fig. 4. In the fluorescence images the ce6 exhibits red fluorescence mainly in the arterial intima and the tissue autofluorescence from the elastic fibers in the arterial media has a yellow color (emission maximum circa 560 nm). There is a small amount of red fluorescence visible from the adventitia which also is known to harbor macrophages.[29] There was a significant correlation between MA-ce6 uptake and RAM-11 staining ($R = 0.83$, $p < 0.001$ Fig. 5(a)). In contrast, there was an inverse correlation between MA-ce6 uptake and smooth muscle cell staining ($R = -0.74$, $p < 0.001$ Fig. 5(b)).

Discussion

These data demonstrate that the fluorescent PDT agent, MA-ce6, localizes within atherosclerotic plaques in proportion to plaque inflammation as measured by macrophage density. Furthermore the data demonstrate that MA-ce6 concentrates within plaques in sufficiently high concentrations to enable intravascular detection of inflamed plaques.

It is well-documented that the majority of infarctions result from the rupture of plaques that in most cases did not cause flow limitations prior to the acute event.[30] An important characteristic of such high-risk/vulnerable plaques (VP) is an abundance of inflammatory cells, which are recognized as playing a central role in plaque disruption.[31] These insights have created an interest in enhancing risk-stratification methods by diagnosing (detecting or imaging) VP.[10,32,33]

Several potential molecular targets exist that may be used to deliver molecular imaging agents to inflammatory cells. Scavenger receptors represent an attractive target for delivering diagnostic or therapeutic molecules to inflamed plaques because of their specificity and high capacity. We have previously demonstrated that the scavenger-receptor-specific PS, MA-ce6, selectively accumulates in macrophages, resulting in approximately 20-fold higher concentration of PS within macrophages compared to other cell lines.[21] In the present report, we demonstrate that MA-ce6 localizes within atherosclerotic plaques, as confirmed by several complementary techniques, including an intravascular detection system. We also show that the degree of MA-ce6 accumulation within the plaques corresponds to the concentration of

macrophages (not to smooth muscle cells). Accordingly, the use of MA-ce6, in conjunction with an intravascular spectrofluorimetry catheter system, may be useful for identifying inflamed atherosclerotic plaques, and differentiating them from smooth muscle-rich plaques.

A report from Nagae et al.[34] showed that MA-ce6 could localize in intimal hyperplastic lesions caused in rats two weeks after balloon injury of the aorta. The rats had received no atherogenic diet and no attempt was made to characterize the cellular components of the lesions, but from literature reports[35] the cells in the lesions might be expected to be proliferative smooth muscle cells rather than activated macrophages. In the present study we found a negative correlation between MA-ce6 fluorescence and smooth muscle cell staining, suggesting that the MA-ce6 conjugate has a much higher affinity for macrophages when they are present due to the higher expression of scavenger receptors on these cells compared to smoothmuscle cells. The high proportion of macrophages in the lesions in the present model, provides additional evidence that the conjugate indeed has the potential to detect these "vulnerable plaques".

The clinical utility of characterizing atherosclerotic plaques according to degree of inflammation remains unproven; it remains to be seen whether such a detection system will improve clinical outcomes in a cost-effective manner. Additionally, several factors require consideration in assessing the prospects for clinical use of this methodology.

Firstly, although the rabbits did not develop noticeable toxicity after exposure to MA-ce6, it should be noted that such preparations might not be pharmacologically neutral. Binding of ligands to the scavenger receptor may lead to macrophage activation and possibly to inflammation.[36] However, data are present to demonstrate tolerability in animal models ranging from rabbits, to mice and guinea pigs.[37,38] Nonetheless, demonstrating that MA-ce6 does not elicit a significant immune response represents a hurdle in moving this technology forward. It should also be noted that SR-A are present in organs of the reticuloendothelial system, especially the liver. Biodistribution data previously revealed[24] that uptake in liver is of the order of 60% (on a tissue weight basis) compared to that found in plaques. However organs such as the liver will receive no light either during detection or during therapy and therefore this uptake is expected to be irrelevant.

Secondly the intravascular detection apparatus employed in this study was not optimized for this application. When we attempted to carry out intravascular fluorescence detection in living rabbits in flowing blood, the values of fluorescence obtained were much reduced in most of the aorta. High fluorescence signals were only obtained when the fiber was advanced up to the aortic arch and came into contact with the artery wall. Therefore we sacrificed the animals before detection. It required gentle pressing of the fiber tip against the vessel to direct the front-viewing catheter towards the vessel wall. In order for eventual clinical use, the catheter will need to be re-designed to enable side-viewing, perhaps using a mirror or prism on the catheter tip to re-direct the light; an approach has been used in other optical catheter technologies.[39]

A third consideration is the possibility that the MA-ce6 can be photoactivated, although this could be avoided by using a non-photosensitizing fluorescent dye attached to maleylated albumin instead of ce6. There have been many advances[40,41] in conjugatable near-infrared fluorescent dyes with much superior optical properties (wavelength, absorption coefficient and fluorescence quantum yield) compared to ce6. The potential for photoactivation with ce6 could require that patients minimize exposure to light during the first several hours after receiving the drug. Moreover, photoactivation opens the possibility of photodynamic therapy (PDT). In this case, PDT using MA-ce6 offers dual selectivity for inflamed plaques: first by virtue of selective accumulation of MA-ce6 within inflamed plaques, second by selective photoactivation of suspicious plaques (a step which requires local, intravascular delivery of light of the appropriate fluence). In fact experiments we have carried out in the present animal

model involving injection of MA-ce6 followed by intra-arterial delivery of therapeutic fluences of 660 nm laser light have shown significant therapeutic reductions in the macrophage content of the illuminated plaques and a manuscript describing these studies is in preparation.

Given the ability to detect inflamed plaques with this technology, the possibility of developing a "seek and destroy" system becomes apparent. The premise of this system is to use a dual function intravascular catheter that first identifies the presence and location of VPs by their fluorescence signal (produced by sending diagnostic light through the fiber). When a VP is detected, the catheter would then have its fiber switched to a light source (probably a laser) to deliver a therapeutic dose of light to the identified VP. Choosing the right combination of light and drug dose will lead to cytotoxicity, which in the case of MA-ce6, will likely result in macrophage apoptosis. Whether this therapeutic effect is clinically desirable remains to be tested. The work of LaMuraglia et al.[42] has shown that carrying out PDT inside arteries does not seem to cause any inflammation or untoward immune response. The reasons for this observation are not entirely clear but appear to be due to the action of blood flow in "washing away" or inactivating any inflammatory mediators that are produced from the dying cells in the artery wall. Clinical studies from Rockson et al.[43] certainly suggest that the intra-arterial PDT procedure will be safe.

Acknowledgments

References

1. Farb A, Tang AL, Burke AP, Sessums L, Liang Y, Virmani R. Sudden coronary death. Frequency of active coronary lesions, inactive coronary lesions, and myocardial infarction. Circulation 1995;92:1701. [PubMed: 7671351]

2. Plutzky J. Atherosclerotic plaque rupture: emerging insights and opportunities. Am. J. Cardiol 1999;84:15J.

3. Arroyo LH, Lee RT. Mechanisms of plaque rupture: mechanical and biologic interactions. Cardiovasc. Res 1999;41:369. [PubMed: 10341836]

4. Castano AP, Demidova TN, Hamblin MR. Mechanisms in photodynamic therapy: part one-photosensitizers, photochemistry and cellular localization. Photodiagn. Photodyn. Ther 2004;1:279.

5. Dougherty TJ. An update on photodynamic therapy applications. J. Clin. Laser Med. Surg 2002;20:3. [PubMed: 11902352]

6. Rockson SG, Lorenz DP, Cheong WF, Woodburn KW. Photoangioplasty: An emerging clinical cardiovascular role for photo-dynamic therapy. Circulation 2000;102:591. [PubMed: 10920074]

7. Jaffer FA, Libby P, Weissleder R. Molecular and cellular imaging of atherosclerosis: emerging applications. J. Am. Coll. Cardiol 2006;47:1328. [PubMed: 16580517]

8. Purushothaman KR, Sanz J, Zias E, Fuster V, Moreno PR. Atherosclerosis neovascularization and imaging. Curr. Mol. Med 2006;6:549. [PubMed: 16918375]

9. Deguchi JO, Aikawa M, Tung CH, Aikawa E, Kim DE, Ntziachristos V, Weissleder R, Libby P. Inflammation in atherosclerosis: visualizing matrix metalloproteinase action in macrophages *in vivo*. Circulation 2006;114:55. [PubMed: 16801460]

10. Rudd JH, Davies JR, Weissberg PL. Imaging of atherosclerosis - can we predict plaque rupture? Trends Cardiovasc. Med 2005;15:17. [PubMed: 15795159]

11. Wagner S, Breyholz HJ, Faust A, Holtke C, Levkau B, Schober O, Schafers M, Kopka K. Molecular imaging of matrix metalloproteinases *in vivo* using small molecule inhibitors for SPECT and PET. Curr. Med. Chem 2006;13:2819. [PubMed: 17073631]

12. Elmaleh DR, Fischman AJ, Tawakol A, Zhu A, Shoup TM, Hoffmann U, Brownell AL, Zamecnik PC. Detection of inflamed atherosclerotic lesions with diadenosine-5′,5‴-P1,P4-tetraphosphate (Ap4A) and positron-emission tomography. Proc. Natl. Acad. Sci. U. S. A 2006;103:15992. [PubMed: 17038498]

13. Amirbekian V, Lipinski MJ, Briley-Saebo KC, Amirbekian S, Aguinaldo JG, Weinreb DB, Vucic E, Frias JC, Hyafil F, Mani V, Fisher EA, Fayad ZA. Detecting and assessing macrophages *in vivo* to evaluate atherosclerosis noninvasively using molecular MRI. Proc. Natl. Acad. Sci. U. S. A 2007;104:961. [PubMed: 17215360]

14. Ntziachristos V, Bremer C, Weissleder R. Fluorescence imaging with near-infrared light: new technological advances that enable *in vivo* molecular imaging. Eur. Radiol 2003;13:195. [PubMed: 12541130]

15. Geng Y, Kodama T, Hansson GK. Differential expression of scavenger receptor isoforms during monocyte-macrophage differentiation and foam cell formation. Arterioscler. Thromb 1994;14:798. [PubMed: 8172856]

16. Freeman MW. Scavenger receptors in atherosclerosis. Curr. Opin. Hematol 1997;4:41. [PubMed: 9050378]

17. Krieger M, Acton S, Ashkenas J, Pearson A, Penman M, Resnick D. Molecular flypaper, host defense, and atherosclerosis. Structure, binding properties, and functions of macrophage scavenger receptors. J. Biol. Chem 1993;268:4569. [PubMed: 8383115]

18. Gough PJ, Greaves DR, Suzuki H, Hakkinen T, Hiltunen MO, Turunen M, Herttuala SY, Kodama T, Gordon S. Analysis of macrophage scavenger receptor (SR-A) expression in human aortic atherosclerotic lesions. Arterioscler. Thromb. Vasc. Biol 1999;19:461. [PubMed: 10073945]

19. Shashkin P, Dragulev B, Ley K. Macrophage differentiation to foam cells. Curr. Pharm. Des 2005;11:3061. [PubMed: 16178764]

20. Yamada Y, Doi T, Hamakubo T, Kodama T. Scavenger receptor family proteins: roles for atherosclerosis, host defence and disorders of the central nervous system. Cell. Mol. Life Sci 1998;54:628. [PubMed: 9711230]

21. Hamblin MR, Miller JL, Ortel B. Scavenger-receptor targeted photodynamic therapy. Photochem. Photobiol 2000;72:533. [PubMed: 11045726]

22. Liu Q, Hamblin MR. Macrophage-targeted photodynamic therapy: scavenger receptor expression and activation state. Int. J. Immunopathol. Pharmacol 2005;18:391. [PubMed: 16164823]

23. Anatelli F, Mroz P, Liu Q, Yang C, Castano AP, Swietlik E, Hamblin MR. Macrophage-targeted photosensitizer conjugate delivered by intratumoral injection. Mol. Pharmacol 2006;3:654.

24. Tawakol A, Castano AP, Anatelli F, Bashian G, Stern J, Zahra T, Gad F, Chirico S, Ahmadi A, Fischman AJ, Muller JE, Hamblin MR. Photosensitizer delivery to vulnerable atherosclerotic plaque: comparison ofmacrophage-targeted conjugate *versus* free chlorine(e6). J. Biomed. Opt 2006;11:21008.

25. Fischman AJ, Lees AM, Lees RS, Barlai-Kovach M, Strauss HW. Accumulation of native and methylated low density lipoproteins by healing rabbit arterial wall. Arteriosclerosis 1987;7:361. [PubMed: 3606463]

26. Puchtler H, Waldrop FS. On the mechanism of Verhoeff's elastica stain: a convenient stain for myelin sheaths. Histochemistry 1979;62:233. [PubMed: 90671]

27. Pocock SJ, Geller NL, Tsiatis AA. The analysis of multiple endpoints in clinical trials. Biometrics 1987;43:487. [PubMed: 3663814]

28. Jackson RA. Interpretation of research data: selected statistical procedures. Am. J. Hosp. Pharm 1980;37:1673. [PubMed: 7446542]

29. Ramshaw AL, Parums DV. Immunohistochemical characterization of inflammatory cells associated with advanced atherosclerosis. Histopathology 1990;17:543. [PubMed: 2076887]

30. Falk E, Shah PK, Fuster V. Coronary plaque disruption. Circulation 1995;92:657. [PubMed: 7634481]

31. Libby P. What have we learned about the biology of atherosclerosis? The role of inflammation. Am. J. Cardiol 2001;88:3J.

32. Fayad ZA, Fuster V. The human high-risk plaque and its detection by magnetic resonance imaging. Am. J. Cardiol 2001;88:42E.

33. Naghavi M, Madjid M, Khan MR, Mohammadi RM, Willerson JT, Casscells SW. New developments in the detection of vulnerable plaque. Curr. Atheroscler. Rep 2001;3:125. [PubMed: 11177656]

34. Nagae T, Louie AY, Aizawa K, Ishimaru S, Wilson SE. Selective targeting and photodynamic destruction of intimal hyperplasia by scavenger-receptor mediated protein-chlorin e6 conjugates. J. Cardiovasc. Surgery 1998;39:709.

35. Law RE, Meehan WP, Xi XP, Graf K, Wuthrich DA, Coats W, Faxon D, Hsueh WA. Troglitazone inhibits vascular smooth muscle cell growth and intimal hyperplasia. J. Clin. Invest 1996;98:1897. [PubMed: 8878442]

36. Hsu HY, Chiu SL, Wen MH, Chen KY, Hua KF. Ligands of macrophage scavenger receptor induce cytokine expression *via* differential modulation of protein kinase signaling pathways. J. Biol. Chem 2001;276:28719. [PubMed: 11390374]

37. Pandey R, Khuller GK. Antitubercular inhaled therapy: opportunities, progress and challenges. J. Antimicrob. Chemother 2005;55:430. [PubMed: 15761077]

38. Srividya S, Roy RP, Basu SK, Mukhopadhyay A. Scavenger receptor-mediated delivery of muramyl dipeptide activates antitumor efficacy of macrophages by enhanced secretion of tumor-suppressive cytokines. J. Leukoc. Biol 2000;67:683. [PubMed: 10811009]

39. Jang IK, Bouma BE, Kang DH, Park SJ, Park SW, Seung KB, Choi KB, Shishkov M, Schlendorf K, Pomerantsev E, Houser SL, Aretz HT, Tearney GJ. Visualization of coronary atherosclerotic plaques in patients using optical coherence tomography: comparison with intravascular ultrasound. J. Am. Coll. Cardiol 2002;39:604. [PubMed: 11849858]

40. Lin Y, Weissleder R, Tung CH. Synthesis and properties of sulfhydryl-reactive near-infrared cyanine fluorochromes for fluorescence imaging. Mol. Imaging 2003;2:87. [PubMed: 12964306]

41. Ye Y, Bloch S, Kao J, Achilefu S. Multivalent carbocyanine molecular probes: synthesis and applications. Bioconjugate Chem 2005;16:51.

42. LaMuraglia GM, Adili F, Karp SJ, Statius van Eps RG, Watkins MT. Photodynamic therapy inactivates extracellular matrix-basic fibroblast growth factor: insights to its effect on the vascular wall. J. Vasc. Surg 1997;26:294. [PubMed: 9279318]

43. Rockson SG, Kramer P, Razavi M, Szuba A, Filardo S, Fitzgerald P, Cooke JP, Yousuf S, DeVault AR, Renschler MF, Adelman DC. Photoangioplasty for human peripheral atherosclerosis: results of a phase I trial of photodynamic therapy with motexafin lutetium (Antrin). Circulation 2000;102:2322. [PubMed: 11067782]
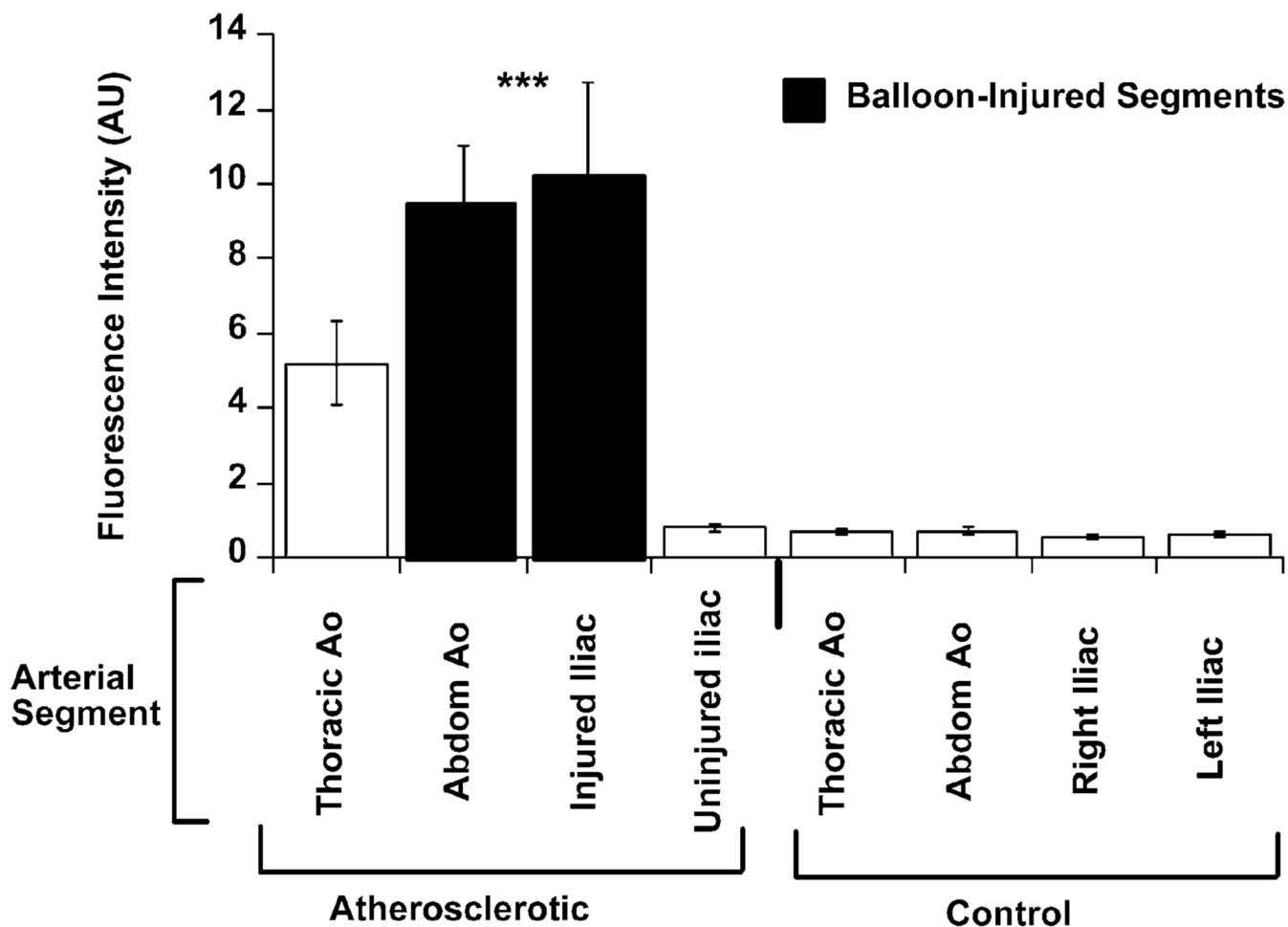
Fig. 1.
Intravascular detection of fluorescence in atherosclerotic and control rabbits. Mean
fluorescence intensity (in arbitrary units ± SD) obtained by the intravascular
spectrofluorimetric catheter. The signal was significantly increased within the aorto-iliac
vessels of atherosclerotic rabbits ($n = 15$) compared to control rabbits ($n = 7, p < 0.001$ ANOVA
atherosclerotic animals *vs.* controls). Note that the signal from balloon-injured iliac arteries of
atherosclerotic animals was approximately 16-times higher than from the contra-lateral iliac
arteries in the same animals, and 24-times higher than the corresponding vessels within control
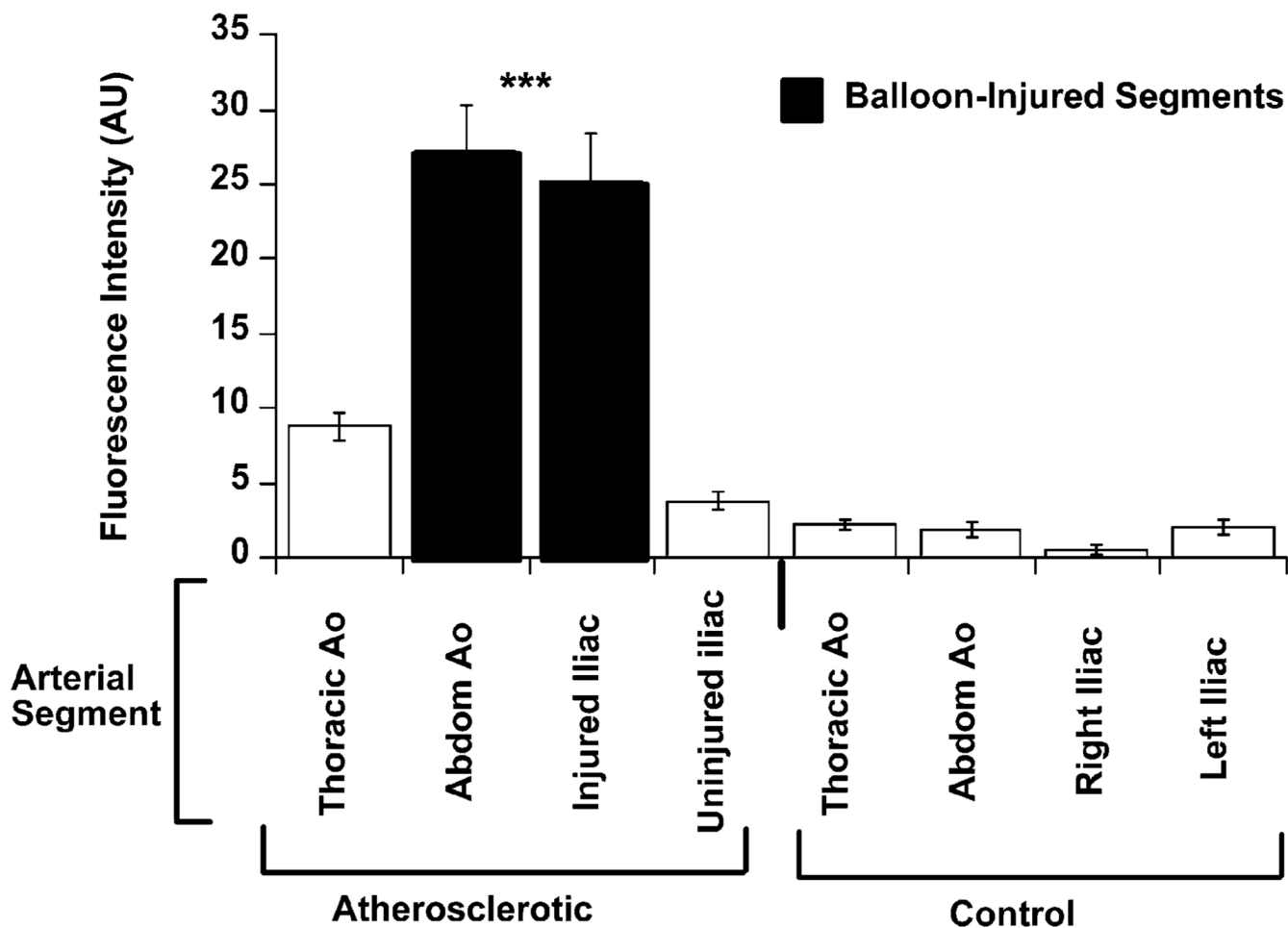animals.

Fig. 2.
Intimal surface fluorescence from atherosclerotic and control aortae. Mean surface
fluorescence intensity (in arbitrary units ± SD) for arterial segments taken from atherosclerotic
and control animals. The spectrofluorimetric signal was significantly increased in the aorto-
iliac vessel of atherosclerotic rabbits ($n = 15$) compared to the corresponding sections of aorta
from control rabbits (n=7, p<0.001 ANOVA atherosclerotic animals *vs.* controls). Note that
the signal from balloon-injured iliac arteries of atherosclerotic animals was approximately 9-
times higher than from the contra-lateral iliac arteries in the same animals, and 21-times higher
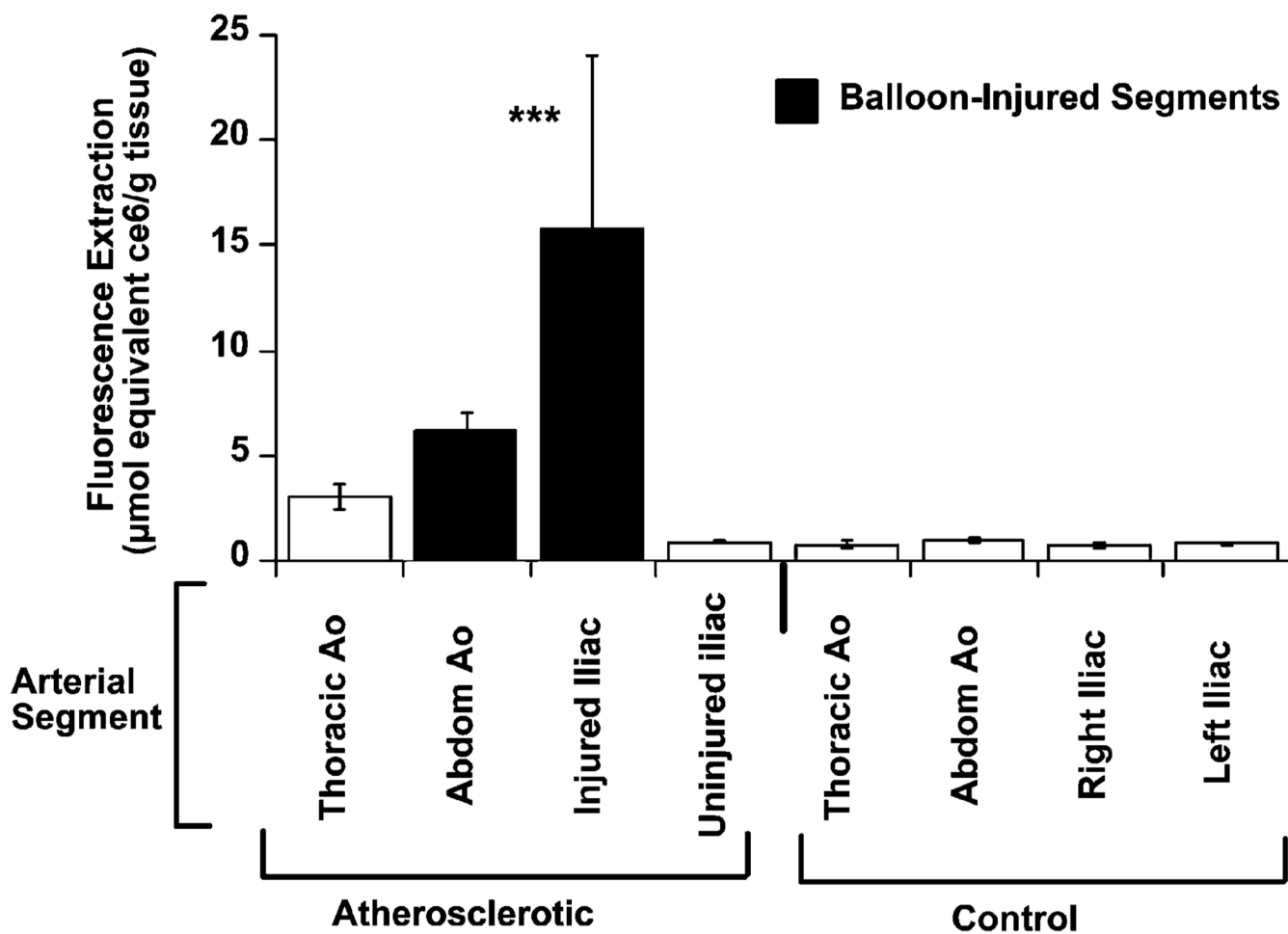than the corresponding vessels within control animals.

Fig. 3.
Fluorescence quantification by extraction from atherosclerotic and control aortae demonstrates the tissue concentration of MA-ce6 (in nmol ce6 equiv (g tissue)$^{-1}$) for arterial segments taken from atherosclerotic and control animals. The tissue concentration of MA-ce6 was significantly increased in all sections from atherosclerotic rabbits compared to the corresponding sections of aorta from control rabbits injected with conjugate ($p < 0.001$ ANOVA atherosclerotic animals *vs.* controls).

Fluorescence Microscopy
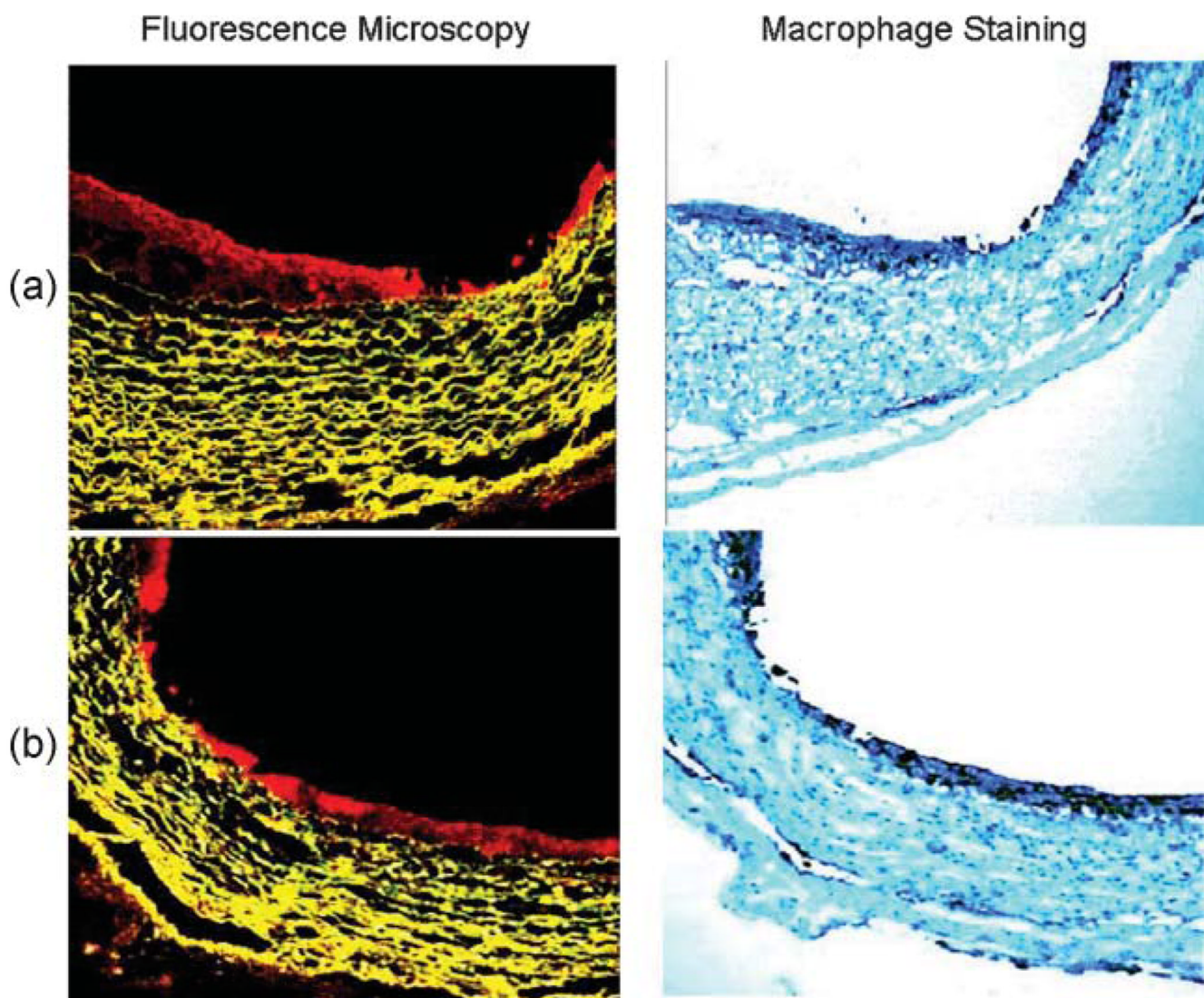
Macrophage Staining

Fig. 4.
Confocal microscopy. Fluorescence micrographs and their corresponding macrophage immunohistochemical staining (RAM-11) in two representative segments (a and b) are shown. In the fluorescence micrographs red fluorescence represents MA-ce6 uptake, whereas in RAM-11 stained images, dark brown staining represents macrophages. In both sets of images, the RAM-11 staining is primarily confined to the intima. MA-ce6 uptake parallels the pattern of RAM-11 staining.
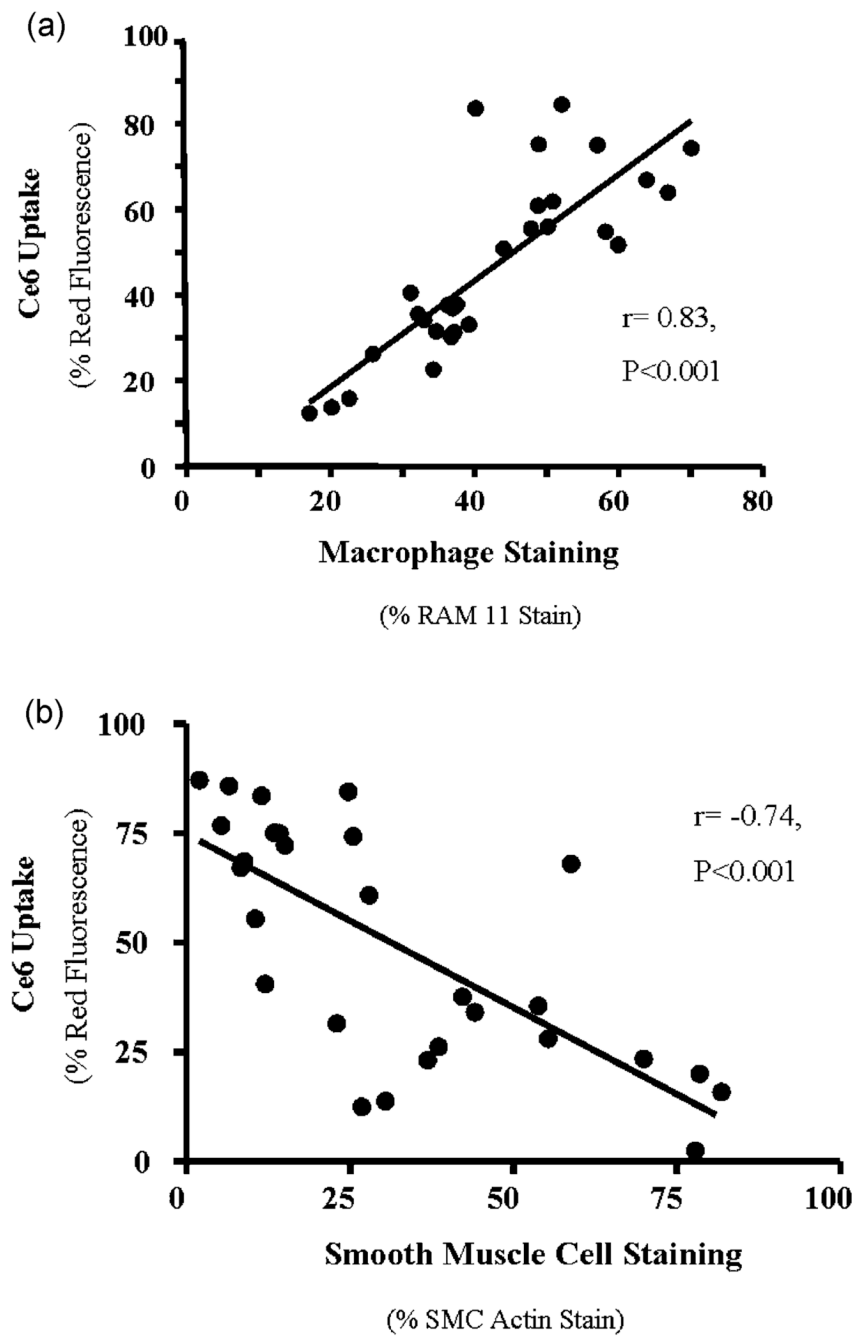
Fig. 5.
Comparison of MA-ce6 uptake *vs.* immnunohistochemical staining. There was a significant correlation between MA-ce6 uptake and RAM-11 staining ((a)R=0.83, $p < 0.001$). In contrast, there was an inverse correlation between MA-ce6 uptake and smooth muscle cell staining ((b) R=−0.74, $p < 0.001$).